

---

# Unsupervised Progressive Learning and the STAM Architecture

---

James Smith   Seth Baer\*   Cameron Taylor\*   Constantine Dovrolis†  
 College of Computing  
 Georgia Institute of Technology  
 Atlanta, GA

## Abstract

We first pose the Unsupervised Progressive Learning (UPL) problem: an online representation learning problem in which the learner observes a non-stationary and unlabeled data stream, and identifies a growing number of features that persist over time even though the data is not stored or replayed. To solve the UPL problem we propose the Self-Taught Associative Memory (STAM) architecture. Layered hierarchies of STAM modules learn based on a combination of online clustering, novelty detection, forgetting outliers, and storing only prototypical features rather than specific examples. We evaluate STAM representations using classification and clustering tasks. Even though there are no prior approaches that are directly applicable to the UPL problem, we evaluate the STAM architecture in comparison to some unsupervised and self-supervised deep learning approaches adapted in the UPL context.

## 1 Introduction

The *Continual Learning (CL)* problem is predominantly addressed in the supervised context with the goal being to learn a sequence of tasks without “catastrophic forgetting” [26, 62, 77]. There are several CL variations but a common formulation is that the learner observes a set of examples  $\{(x_i, t_i, y_i)\}$ , where  $x_i$  is a feature vector,  $t_i$  is a task identifier, and  $y_i$  is the target vector associated with  $(x_i, t_i)$  [9, 10, 55]. Other CL variations replace task identifiers with task boundaries that are either given [31] or inferred [85]. Typically, CL requires that the learner either stores and replays some previously seen examples [2, 3, 22, 27, 37, 67] or generates examples of earlier learned tasks [36, 52, 71].

The *Feature (or Representation) Learning (FL)* problem, on the other hand, is unsupervised but mostly studied in the *offline context*: given a set of examples  $\{x_i\}$ , the goal is to learn a *feature vector* (of a given, fixed dimensionality)  $h_i = f(x_i)$  that, ideally, makes it easier to identify the explanatory factors of variation behind the data [5], leading to better performance in tasks such as classification or clustering. FL methods differ in the prior  $P(h)$  and the loss function. Autoencoders, for instance, aim to learn features of a lower dimensionality than the input that enable a sufficiently good reconstruction at the output [4, 40, 76, 86]. A similar approach is self-supervised methods, which learn representations by optimizing an auxiliary task [6, 17, 23, 45, 60, 73].

In this work, we focus on a new and pragmatic problem that adopts some elements of CL and FL but is also different than them – we refer to this problem as *Unsupervised Progressive Learning (UPL)*. UPL can be described as follows:

1. the data is observed as a non-IID stream (e.g., different portions of the stream may follow different distributions and there may be strong temporal correlations between successive examples),

---

\*equal contribution

†Correspondence to: Constantine Dovrolis <constantine@gatech.edu>

2. the features should be learned exclusively from unlabeled data,
3. each example is “seen” only once and the unlabeled data are not stored for iterative processing,
4. the number of learned features may need to increase over time, in response to new tasks and/or changes in the data distribution,
5. to avoid catastrophic forgetting, previously learned features need to persist over time, even when the corresponding data are no longer observed in the stream.

The UPL problem is encountered in important AI applications, such as a robot learning new visual features as it explores a time-varying environment. Additionally, we argue that UPL is closer to how animals learn, at least in the case of *perceptual learning* [24]. We believe that in order to mimic that, ML methods should be able to learn in a streaming manner and in the absence of supervision. Animals do not “save off” labeled examples to train in parallel with unlabeled data, they do not know how many “classes” exist in their environment, and they do not have to replay/dream periodically all their past experiences to avoid forgetting them.

To the extent of our knowledge, the UPL problem has not been addressed before. The closest prior work is CURL (“Continual Unsupervised Representation Learning”) by Rao et al. [65]. CURL however does not impose the requirement that the data is presented to the learner as a stream that should be processed online, and so CURL requires iterative processing through gradient minimization methods (additional differences with CURL are discussed in Section 6).

To address the UPL problem, we describe an architecture referred to as STAM (“Self-Taught Associative Memory”). STAM learns features through *online clustering* at a hierarchy of increasing receptive field sizes. Online clustering can be performed through a single pass over the data stream. Further, despite its simplicity, clustering can generate representations that enable better classification performance than more complex FL methods such as sparse-coding or some deep learning methods [12, 13]. STAM allows the number of clusters to increase over time, driven by a *novelty detection* mechanism. Additionally, STAM includes a brain-inspired *dual-memory hierarchy* (short-term versus long-term) that enables the conservation of previously learned features (to avoid catastrophic forgetting) that have been seen multiple times at the data stream, while forgetting outliers.

## 2 STAM Architecture

In the following, we describe the STAM architecture as a sequence of its major components: a hierarchy of increasing receptive fields, online clustering (centroid learning), novelty detection, and a dual-memory hierarchy that stores prototypical features rather than specific examples. The notation is summarized for convenience in the Supplementary Material section SM-A.

**I. Hierarchy of increasing receptive fields:** An input vector  $\mathbf{x}_t \in \mathbb{R}^n$  (an image in all subsequent examples) is analyzed through a hierarchy of  $\Lambda$  layers. Instead of neurons or hidden-layer units, each layer consists of STAM units – in its simplest form a STAM unit functions as an online clustering module. Each STAM processes one  $\rho_l \times \rho_l$  *patch* (subvector) of the input at that layer. The patches are overlapping, with a small stride (set to one pixel in our experiments) to accomplish translation invariance (similar to CNNs). The patch dimension  $\rho_l$  increases in higher layers – the idea is that the first layer learns the smallest and most elementary features while the top layer learns the largest and most complex features.

**II. Centroid Learning:** Every patch of each layer is clustered, in an online manner, to a set of centroids. These time-varying centroids form the *features* that the STAM architecture gradually learns at that layer. All STAM units of layer  $l$  share the same set of centroids  $C_l(t)$  – again for translation invariance.<sup>3</sup> Given the  $m$ ’th input patch  $\mathbf{x}_{1,m}$  at layer  $l$ , the nearest centroid of  $C_l$  selected for  $\mathbf{x}_{1,m}$  is

$$\mathbf{c}_{1,j} = \arg \min_{\mathbf{c} \in C_l} d(\mathbf{x}_{1,m}, \mathbf{c}) \quad (1)$$

where  $d(\mathbf{x}_{1,m}, \mathbf{c})$  is the Euclidean distance between the patch  $\mathbf{x}_{1,m}$  and centroid  $\mathbf{c}$ .<sup>4</sup> The selected centroid is updated based on a learning rate parameter  $\alpha$ , as follows:

$$\mathbf{c}_{1,j} = \alpha \mathbf{x}_{1,m} + (1 - \alpha) \mathbf{c}_{1,j}, \quad 0 < \alpha < 1 \quad (2)$$

<sup>3</sup>We drop the time index  $t$  from this point on but it is still implied that the centroids are dynamically learned over time.

<sup>4</sup>We have also experimented with the L1 metric with only minimal differences. Different distance metrics may be more appropriate for other types of data.

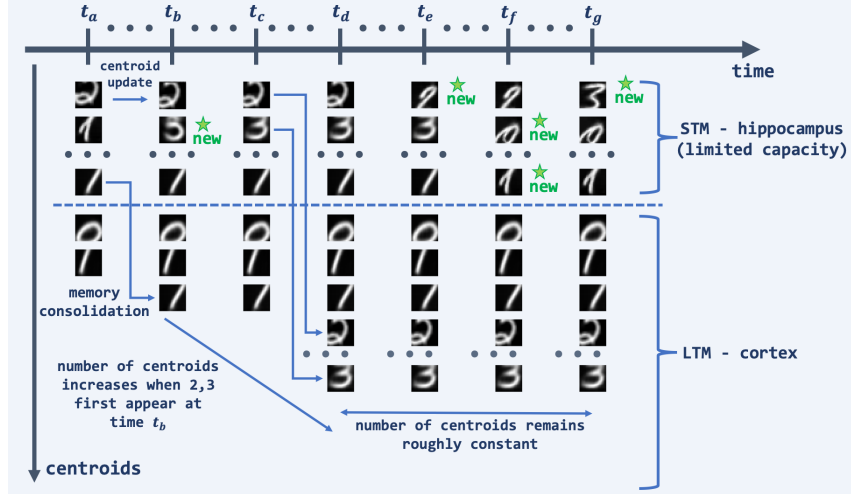


**Figure 1:** A hypothetical pool of STM and LTM centroids visualized at seven time instants. From  $t_a$  to  $t_b$ , a centroid is moved from STM to LTM after it has been selected  $\theta$  times. At time  $t_b$ , unlabeled examples from classes ‘2’ and ‘3’ first appear, triggering novelty detection and new centroids are created in STM. These centroids are moved into LTM by  $t_d$ . From  $t_d$  to  $t_g$ , the pool of LTM centroids remains the same because no new classes are seen. The pool of STM centroids keeps changing when we receive “outlier” inputs of previously seen classes. Those centroids are later replaced (Least-Recently-Used policy) due to the limited capacity of the STM pool.

A higher  $\alpha$  value makes the learning process faster but less predictable. We do not use a decreasing value of  $\alpha$  because the goal is to keep learning in a non-stationary environment rather than convergence to a stable centroid.

**III. Novelty detection:** When an input patch  $\mathbf{x}_{l,m}$  at layer  $l$  is significantly different than all centroids at that layer (i.e., its distance to the nearest centroid is a statistical outlier), a new centroid is created in  $C_l$  based on  $\mathbf{x}_{l,m}$ . We refer to this event as *Novelty Detection (ND)*. This function is necessary so that the architecture can learn novel features when the data distribution changes.

To do so, we estimate in an online manner the distance distribution between input patches and their nearest centroid (separately for each layer). The novelty detection threshold at layer  $l$  is denoted by  $\hat{D}_l$  and it is defined as the 95-th percentile ( $\beta = 0.95$ ) of this distance distribution.

**IV. Dual-memory organization:** New centroids are stored temporarily in a *Short-Term Memory (STM)* of limited capacity  $\Delta$ , separately for each layer. Every time a centroid is selected as the nearest neighbor of an input patch, it is updated based on (2). If an STM centroid  $\mathbf{c}_{l,j}$  is selected more than  $\theta$  times, it is copied to the *Long-Term Memory (LTM)* for that layer. We refer to this event as *memory consolidation*. The LTM has (practically) unlimited capacity and the learning rate is much smaller (in our experiments the LTM learning rate is set to zero).

This memory organization is inspired by the Complementary Learning Systems framework [44], where the STM role is played by the hippocampus and the LTM role by the cortex. This dual-memory scheme is necessary to distinguish between infrequently seen patterns that can be forgotten (“outliers”), and new patterns that are frequently seen after they first appear (“novelty”).

We initialize the pool of STM centroids at each layer using randomly sampled patches from the first few images of the unlabeled stream. When the STM pool of centroids at a layer is full, the introduction of a new centroid (created through novelty detection) causes the removal of an earlier centroid. We use the Least-Recently Used (LRU) policy to remove atypical centroids that have not been recently selected by any input. Figure 1 illustrates this dual-memory organization.

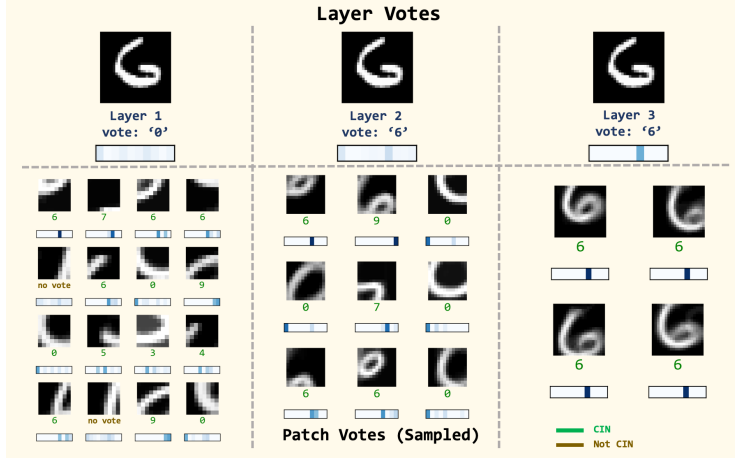


**Figure 2:** An example of the classification process. Every patch (at any layer) that selects a CIN centroid votes for the single class that has the highest association with. These patch votes are first averaged at each layer. The final inference is the class with the highest cumulative vote across all layers.

### 3 Classification using STAM

Given a small amount of labeled data, STAM can be used in classification tasks. We emphasize that the labeled data is not used for representation learning – it is only used to associate previously learned features with a given set of classes.

**I. Associating centroids with classes:** Suppose we are given some labeled examples  $X_L(t)$  from a set of classes  $L(t)$  at time  $t$ . We can use these labeled examples to associate existing LTM centroids at time  $t$  (learned strictly from unlabeled data) with the set of classes in  $L(t)$ .

Given a labeled example of class  $k$ , suppose that there is a patch  $\mathbf{x}$  in that example for which the nearest centroid is  $\mathbf{c}$ . That patch contributes the following association between centroid  $\mathbf{c}$  and class  $k$ :

$$f_{\mathbf{x},\mathbf{c}}(k) = e^{-d(\mathbf{x},\mathbf{c})/\bar{D}_t} \quad (3)$$

where  $\bar{D}_t$  is a normalization constant (calculated as the average distance between input patches and centroids).

The *class-association vector*  $\mathbf{g}_{\mathbf{c}}$  between centroid  $\mathbf{c}$  and any class  $k$  is computed aggregating all such associations, across all labeled examples in  $X_L$ :

$$g_{\mathbf{c}}(k) = \frac{\sum_{\mathbf{x} \in X_L(k)} f_{\mathbf{x},\mathbf{c}}(k)}{\sum_{k' \in L(t)} \sum_{\mathbf{x} \in X_L(k')} f_{\mathbf{x},\mathbf{c}}(k')}, \quad k = 1 \dots L(t) \quad (4)$$

where  $X_L(k)$  refers to labeled examples belonging to class  $k$ . Note that  $\sum_k g_{\mathbf{c}}(k) = 1$ .

**II. Class informative centroids:** If a centroid is associated with only one class  $k$  ( $g_{\mathbf{c}}(k) = 1$ ), only labeled examples of that class select that centroid. At the other extreme, if a centroid is equally likely to be selected by examples of any labeled class, ( $g_{\mathbf{c}}(k) \approx 1/|L(t)|$ ), the selection of that centroid does not provide any significant information for the class of the corresponding input. We identify the centroids that are *Class Informative (CIN)* as those that are associated with at least one class significantly more than expected by chance. Specifically, a centroid  $\mathbf{c}$  is CIN if

$$\max_{k \in L(t)} g_{\mathbf{c}}(k) > \frac{1}{|L(t)|} + \gamma \quad (5)$$

where  $\frac{1}{|L(t)|}$  is the chance term and  $\gamma$  is the significance term.

**III. Classification using a hierarchy of centroids:** At test time, we are given an input  $\mathbf{x}$  of class  $k(\mathbf{x})$  and infer its class as  $\hat{k}(\mathbf{x})$ . The classification task is a “biased voting” process in which every patch of  $\mathbf{x}$ , at any layer, votes for a single class as long as that patch selects a CIN centroid.

Specifically, if a patch  $\mathbf{x}_{l,m}$  of layer  $l$  selects a CIN centroid  $\mathbf{c}$ , then that patch votes  $v_{l,m}(k) = \max_{k \in L(t)} g_{\mathbf{c}}(k)$  for the class  $k$  that has the highest association with  $\mathbf{c}$ , and zero for all other classes. If  $c$  is *not* a CIN centroid, the vote of that patch is  $v_{l,m}(k) = 0$  for all classes.

The vote of layer  $l$  for class  $k$  is the average vote across all patches in layer  $l$  (as illustrated in Figure 2):

$$v_l(k) = \frac{\sum_{m \in M_l} v_{l,m}(k)}{|M_l|} \quad (6)$$

where  $M_l$  is the set of patches in layer  $l$ . The final inference for input  $\mathbf{x}$  is the class with the highest cumulative vote across all layers:

$$\hat{k}(\mathbf{x}) = \arg \max_{k'} \sum_{l=1}^{\Lambda} v_l(k) \quad (7)$$

## 4 Clustering using STAM

We can also use STAM representations in unsupervised tasks, such as offline clustering. To do this, we first define an embedding function that maps a given vector  $\mathbf{x}$  into the space defined by STAM LTM centroids. In particular, the embedding is defined as  $\Phi(\mathbf{x}) : \mathbb{R}^n \rightarrow \mathbb{R}^{|C|}$ , where the element  $j = 1 \dots |C|$  of  $\Phi(\mathbf{x})$  is the normalized distance (Equation (3)) between the LTM centroid  $c_j$  and its *closest patch* in  $\mathbf{x}$ . The embedding vector represents how strongly each feature (LTM centroid) is present anywhere in the given input. The embedding vectors of a given dataset are then clustered offline using  $k$ -means for a given value of  $k$ . Any other clustering algorithm could be used instead.

## 5 Evaluation

To evaluate the STAM architecture in the UPL context, we consider a data stream in which small groups of classes appear in successive *phases*, referred to as **Incremental UPL**. New classes are introduced two at a time in each phase, and they are only seen in that phase. STAM must be able to both recognize new classes when they are first seen in the stream, and to also remember all previously learned classes without catastrophic forgetting.

Another evaluation scenario is **Uniform UPL**, where all classes appear with equal probability throughout the stream. The results for Uniform UPL are shown in section SM-F.

For brevity, we include results for three datasets: MNIST [46], EMNIST (balanced split with 47 classes) [14], and SVHN [58] (we have also experimented with CIFAR). For each dataset we utilize the standard training and test splits. We preprocess the images by applying per-patch normalization (instead of image normalization), and color images are transformed to grayscale. More information about the image preprocessing can be found in section SM-G.

We create the training stream by randomly selecting, with equal probability,  $N_p$  data examples from the classes seen during each phase.  $N_p$  is set to 8000, 8000, and 2000 for MNIST, SVHN, and EMNIST respectively. More information about the impact of the stream size can be found in section SM-D.

In the classification task, we select a small portion of the training dataset as the labeled examples that are available only to the classifier.

In each task, we average results over three different unlabeled data streams. During testing, we select 100 random examples of each class from the test dataset. This process is repeated five times for each training stream (i.e., a total of fifteen results per experiment). The following plots show mean  $\pm$  standard deviation ranges.

We utilize one F72s V2 and one NC6s V2 virtual machine from Microsoft’s Azure cloud computing service to perform all experiments.

For all datasets, we use a 3-layer STAM hierarchy. The hyperparameter values are tabulated in section SM-A. The robustness of the results with respect to these values is shown in section SM-E.

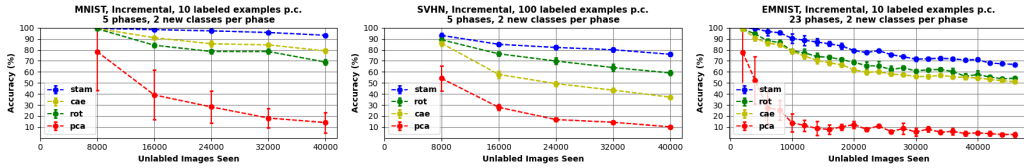


**Figure 3:** Classification accuracy for MNIST (left), SVHN (center), and EMNIST (right). The task is expanding classification for incremental UPL, i.e., recognize all classes seen so far. Note that the number of labeled examples is 10 per class for MNIST and EMNIST and 100 per class for SVHN.

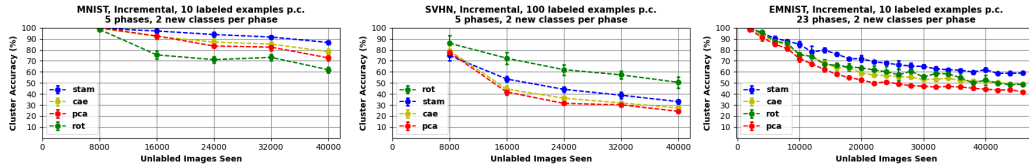


**Figure 4:** Clustering accuracy for MNIST (left), SVHN (center), and EMNIST (right). The task is expanding clustering for incremental UPL. The number of clusters is equal to the number of classes in the data stream seen up to that point in time.

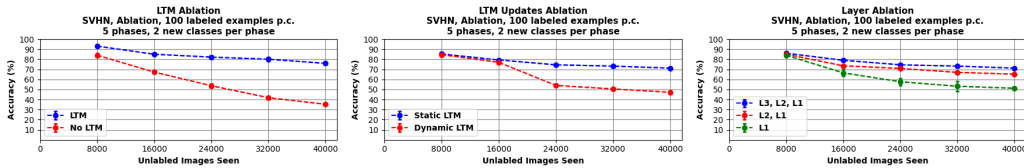


**Figure 5:** Ablation study: A STAM architecture without LTM (left), a STAM architecture in which the LTM centroids are adjusted with the same learning rate  $\alpha$  as in STM (center), and a STAM architecture with removal of layers (right)

**Baseline Methods:** We evaluate the STAM architecture comparing its performance to few basic unsupervised and self-supervised models that we have adapted in the UPL context. We emphasize that there are no prior approaches that are directly applicable to the UPL problem, and so we cannot perform direct comparisons between STAM and “competing” models. In follow-up work, we plan to modify existing methods that were designed to address different problems (such as CURL, GEM or iCURL) in the UPL context and compare them with STAM. The baselines we consider here are:

- (I) a **Convolutional AutoEncoder (CAE)** trained to minimize Euclidean reconstruction error,
- (II) a **rotation-based self-supervised method** which learns the auxiliary task of predicting image rotations based on *RotNet* [23], and
- (III) **offline Principal Component Analysis (PCA)**, just for reference purposes, as it is probably the simplest baseline.

A detailed description of these baseline models is presented in section SM-B.

To satisfy the stream requirement of UPL, the number of training epochs for the CAE and RotNet models is set to one. This is necessary so that each unlabeled example is processed only once. Deep learning methods become weaker in this streaming scenario because they cannot train iteratively over several epochs on the same dataset. For all baselines, the classification task is performed using a  $K$  nearest-neighbor (KNN) classifier – we have experimented with various values of  $K$  and other single-pass classifiers, and report only the best performing results here.

We have also compared the memory requirement of STAM (storing centroids at STM and LTM) with the memory requirement of the CAE and RotNet baselines (storing neural network weights). The results of that comparison appear in section SM-H. For instance, STAM has 17% of RotNet’s memory footprint.

**Classification Task:** We focus on an *expanding classification task*, meaning that in each phase we need to classify *all* classes seen so far. The results for the classification task are given in Figure 3.

Note that we use only 10 labeled examples per class for MNIST and EMNIST, and 100 examples per class for SVHN.

As we introduce new classes in the training stream, the average accuracy per phase decreases for all methods in each dataset. This is expected, as the task gets *more difficult* after each phase. We focus on which method performs best in each task, and which methods see a smaller decrease in accuracy per phase. In the first dataset (MNIST), we observe that STAM performs consistently better than RotNet and CAE, and STAM is less vulnerable to catastrophic forgetting. For SVHN, the trend is similar after the first phase but the difference between STAM and RotNet is much smaller. Finally, in EMNIST, we see a consistently higher accuracy with STAM compared to the deep learning baselines. For additional analysis and discussion of these results, please also refer to section SM-C.

**Clustering Task:** Given that we have the same number of test vectors per class, we associate each cluster with the most-represented class in that cluster. Any instances of another class in that cluster are counted as errors. The number of clusters  $k$  is equal to twice the number of classes seen up to that phase in the unlabeled datastream. The results of the clustering task are given in Figure 4.

For MNIST, STAM still performs consistently better than the two other models, and its accuracy stays almost constant going from 4 classes to 10 classes. For SVHN, RotNet performs significantly better. Finally, for EMNIST, STAM outperforms the two deep learning methods without experiencing significant loss of accuracy after the first 10 phases (20 classes).

**Ablation studies:** Several STAM ablations are presented in Figure 5. On the left, we remove the LTM capability and only use STM centroids for classification. During the first two phases, there is little (if any) difference in classification accuracy. However, we see a clear dropoff during phases 3-5. This suggests that, without the LTM mechanisms, features from classes that are no longer seen in the stream are forgotten over time, and STAM can only successfully classify classes that have been recently seen.

We also investigate the importance of having static LTM centroids rather than dynamic centroids (Fig. 5-middle). Specifically, we replace the static LTM with a dynamic LTM in which the centroids are adjusted with the same learning rate parameter  $\alpha$ , as in STM. The accuracy suffers drastically because the introduction of new classes “takes over” LTM centroids of previously learned classes, after the latter are removed from the stream. Similar to the removal of LTM, we do not see the effects of “forgetting” until phases 3-5. Note that the degradation due to a dynamic LTM is less severe than that from removing LTM completely.

Finally, we look at the effects of removing layers from the STAM hierarchy (Fig. 5-right). We see a small drop in accuracy after removing layer 3, and a large drop in accuracy after also removing layer 2. The importance of having a deeper hierarchy would be more pronounced in datasets with higher-resolution images or videos, potentially showing multiple objects in the same frame. In such cases, CIN centroids can appear at any layer, starting from the lowest to the highest.

**Additional results:** The reader can find additional experimental results in the Supp-Material section that focus on the questions: how does the number of LTM centroids increase with time and what fraction of them are “Class Informative” (in classification tasks), how does the accuracy of STAM vary with the number of labeled examples per class, and how do the various hyperparameters of the STAM architecture affect classification accuracy?

## 6 Related Work

The UPL problem has some similarities with several recent approaches in the machine learning literature but it is also different in important aspects we describe in this section. Each paragraph highlights the most relevant prior work and explains how it is different from UPL.

**I: Continual learning:** In addition to CL models cited in the introduction, other *supervised* CL methods include regularization-based approaches [1, 25, 28, 41, 82, 84], expanding architectures [53, 56, 70], and distillation-based methods [48, 49, 51]. Their main difference with UPL and STAM is that they are designed for supervised learning, and it is not clear how to adapt them for non-stationary and unlabeled data streams.

**II. Offline unsupervised learning:** Additional *offline* representation learning methods include clustering [8, 34, 79, 80], generative models [19, 35, 42, 43], information theory [30, 33], among others. These methods require prior information about the number of classes present in a given dataset (to set the number of cluster centroids or class outputs) and iterative training (i.e. data replay), and therefore cannot be directly applied in the UPL setting.

**III. Semi-supervised learning (SSL):** SSSL methods require labeled data during the representation learning stage and so they are not compatible with UPL [39, 47, 57, 59, 66, 74, 75].

**IV. Few-shot learning (FSL) and Meta-learning:** These methods recognize object classes not seen in the training set with only a single (or handful) of labeled examples [20, 21, 68, 72]. Similar to SSL, FSL methods require labeled data to learn representations and therefore are not applicable in the UPL context. Centroid networks [32] do not require labeled examples at inference time but require labeled examples for training.

**V. Multi-Task Learning (MTL):** Any MTL method that involves separate heads for different tasks is not compatible with UPL because task boundaries are not known a priori in UPL [69]. MTL methods that require pre-training on a large labeled dataset are also not applicable to UPL [61, 83].

**VI. Online and Progressive Learning:** Many earlier methods learn in an online manner, meaning that data is processed in fixed batches and discarded afterwards. This includes progressive learning [78] and streaming with limited supervision [11, 50, 54], both of which require labeled data in the training stream.

**VII. Continual Unsupervised Representation Learning (CURL):** Similar to STAM, CURL also focuses on the problem of continual unsupervised learning from non-stationary data with unknown task boundaries [65]. Its main difference with STAM however is that it is not a streaming method, and so it does not require that each example is seen only once. The CURL model requires gradient-based optimization, going through the same data multiple times. Another difference with STAM is that catastrophic forgetting in CURL is addressed through a generative model that also needs to be learned.

**VIII. Data dimensionality and clustering-based representation learning:** As mentioned earlier in this section, clustering has been used successfully in the past for offline representation learning (e.g., [12, 13]). Its effectiveness, however, gradually drops as the input dimensionality increases [7, 29]. In the STAM architecture, we avoid this issue by clustering smaller subvectors (patches) of the input data. If those subvectors are still of high dimensionality, another approach is to reduce the *intrinsic dimensionality* of the input data at each layer by reconstructing that input using representations (selected centroids) from the previous layer.

**VIII. Related work to other STAM components:** STAM relies on online clustering. This algorithm can be implemented with a rather simple recurrent neural network of excitatory and inhibitory spiking neurons, as shown recently [64]. The novelty detection component of STAM is related to the problem of anomaly detection in streaming data [16] — and the simple algorithm currently in STAM can be replaced with more sophisticated methods (e.g., [15, 81]). Finally, brain-inspired dual-memory systems have been proposed before for memory consolidation (e.g., [36, 63, 71]).

## 7 Discussion

The STAM architecture aims to address the following desiderata that is often associated with Lifelong Learning [62]:

**I. Online learning:** STAMs update the learned features with every observed example. There is no separate training stage for specific tasks, and inference can be performed in parallel with learning.

**II. Transfer learning:** The features learned by the STAM architecture in earlier phases can be also encountered in the data of future tasks (forward transfer). Additionally, new centroids committed to LTM can also be closer to data of earlier tasks (backward transfer).

**III. Resistance to catastrophic forgetting:** The STM-LTM memory hierarchy of the STAM architecture mitigates catastrophic forgetting by committing to "permanent storage" (LTM) features that have been often seen in the data during any time period of the training period.

**IV. Expanding learning capacity:** The unlimited capacity of LTM allows the system to gradually learn more features as it encounters new classes and tasks. The relatively small size of STM, on the



other hand, forces the system to forget features that have not been recalled frequently enough after their creation.

**V. No direct access to previous experience:** STAM only needs to store data centroids in a hierarchy of increasing receptive fields – there is no need to store previous exemplars or to learn a generative model that can produce such examples.

## 8 Broader Impact

We hope that the proposed problem (UPL) and architecture (STAM) will attract the ML community’s interest in streaming-based continual learning without supervision. There is a wide range of applications that fall in that learning paradigm, including autonomous vehicles, live event surveillance, and online trading. We should note that the original insights behind the STAM architecture were inspired by neuroscience. Our hypothesis has been that cortical columns perform some form of online clustering, similar to STAM modules [18].

Unlike deep learning models, the STAM features are highly interpretable (they show prototypical patterns of the input stream). Therefore, improper use of the model parameters can violate user data privacy. We recommend that the model is treated with the same privacy restrictions as the data stream it is trained on.

## Acknowledgements

This work is supported by the Lifelong Learning Machines (L2M) program of DARPA/MTO: Cooperative Agreement HR0011-18-2-0019. The authors acknowledge the comments of Zsolt Kira for an earlier version of this work.

## References

- [1] Rahaf Aljundi, Francesca Babiloni, Mohamed Elhoseiny, Marcus Rohrbach, and Tinne Tuytelaars. Memory aware synapses: Learning what (not) to forget. In *ECCV*, 2018.
- [2] Rahaf Aljundi, Eugene Belilovsky, Tinne Tuytelaars, Laurent Charlin, Massimo Caccia, Min Lin, and Lucas Page-Caccia. Online continual learning with maximal interfered retrieval. In *Advances in Neural Information Processing Systems*, pages 11849–11860, 2019.
- [3] Rahaf Aljundi, Min Lin, Baptiste Goujaud, and Yoshua Bengio. Gradient based sample selection for online continual learning. In *Advances in Neural Information Processing Systems*, pages 11816–11825, 2019.
- [4] Yoshua Bengio. How auto-encoders could provide credit assignment in deep networks via target propagation. *arXiv preprint arXiv:1407.7906*, 2014.
- [5] Yoshua Bengio, Aaron Courville, and Pascal Vincent. Representation learning: A review and new perspectives. *IEEE Trans. Pattern Anal. Mach. Intell.*, 35(8):1798–1828, August 2013.
- [6] David Berthelot, Nicholas Carlini, Ian Goodfellow, Nicolas Papernot, Avital Oliver, and Colin A Raffel. Mixmatch: A holistic approach to semi-supervised learning. In *Advances in Neural Information Processing Systems*, pages 5050–5060, 2019.
- [7] Kevin S. Beyer, Jonathan Goldstein, Raghu Ramakrishnan, and Uri Shaft. When is “nearest neighbor” meaningful? In *Proceedings of the 7th International Conference on Database Theory, ICDT ’99*, pages 217–235, London, UK, UK, 1999. Springer-Verlag.
- [8] Mathilde Caron, Piotr Bojanowski, Armand Joulin, and Matthijs Douze. Deep clustering for unsupervised learning of visual features. In *The European Conference on Computer Vision (ECCV)*, September 2018.
- [9] Arslan Chaudhry, Marc’Aurelio Ranzato, Marcus Rohrbach, and Mohamed Elhoseiny. Efficient lifelong learning with a-GEM. In *International Conference on Learning Representations*, 2019.

- [10] Arslan Chaudhry, Marcus Rohrbach, Mohamed Elhoseiny, Thalaiyasingam Ajanthan, Puneet K Dokania, Philip HS Torr, and Marc Aurelio Ranzato. Continual learning with tiny episodic memories. *arXiv preprint arXiv:1902.10486*, 2019.
- [11] Ioannis Chiotellis, Franziska Zimmermann, Daniel Cremers, and Rudolph Triebel. Incremental semi-supervised learning from streams for object classification. In *2018 IEEE/RSJ International Conference on Intelligent Robots and Systems (IROS)*, pages 5743–5749. IEEE, 2018.
- [12] Adam Coates, Andrew Ng, and Honglak Lee. An analysis of single-layer networks in unsupervised feature learning. In *Proceedings of the fourteenth international conference on artificial intelligence and statistics*, pages 215–223, 2011.
- [13] Adam Coates and Andrew Y Ng. *Learning feature representations with k-means*, pages 561–580. Springer, 2012.
- [14] Gregory Cohen, Saeed Afshar, Jonathan Tapson, and André van Schaik. Emnist: an extension of mnist to handwritten letters. *ArXiv*, abs/1702.05373, 2017.
- [15] Yuwei Cui, Subutai Ahmad, and Jeff Hawkins. Continuous online sequence learning with an unsupervised neural network model. *Neural Comput.*, 28(11):2474–2504, November 2016.
- [16] Sanjoy Dasgupta, Timothy C Sheehan, Charles F Stevens, and Saket Navlakha. A neural data structure for novelty detection. *Proceedings of the National Academy of Sciences*, 115(51):13093–13098, 2018.
- [17] Carl Doersch, Abhinav Gupta, and Alexei A. Efros. Unsupervised visual representation learning by context prediction. *2015 IEEE International Conference on Computer Vision (ICCV)*, pages 1422–1430, 2015.
- [18] Constantine Dovrolis. A neuro-inspired architecture for unsupervised continual learning based on online clustering and hierarchical predictive coding, 2018.
- [19] S. M. Ali Eslami, Nicolas Heess, Theophane Weber, Yuval Tassa, David Szepesvari, Koray Kavukcuoglu, and Geoffrey E. Hinton. Attend, infer, repeat: Fast scene understanding with generative models. In *Proceedings of the 30th International Conference on Neural Information Processing Systems, NIPS’16*, pages 3233–3241, USA, 2016. Curran Associates Inc.
- [20] Li Fei-Fei, R. Fergus, and P. Perona. One-shot learning of object categories. *IEEE Transactions on Pattern Analysis and Machine Intelligence*, 28(4):594–611, April 2006.
- [21] Chelsea Finn, Pieter Abbeel, and Sergey Levine. Model-agnostic meta-learning for fast adaptation of deep networks. In *Proceedings of the 34th International Conference on Machine Learning - Volume 70, ICML’17*, pages 1126–1135. JMLR.org, 2017.
- [22] Alexander Gepperth and Cem Karaoguz. Incremental learning with self-organizing maps. *2017 12th International Workshop on Self-Organizing Maps and Learning Vector Quantization, Clustering and Data Visualization (WSOM)*, pages 1–8, 2017.
- [23] Spyros Gidaris, Praveer Singh, and Nikos Komodakis. Unsupervised representation learning by predicting image rotations. In *International Conference on Learning Representations*, 2018.
- [24] Robert L Goldstone. Perceptual learning. *Annual review of psychology*, 49(1):585–612, 1998.
- [25] Siavash Golkar, Michael Kagan, and Kyunghyun Cho. Continual learning via neural pruning. *arXiv preprint arXiv:1903.04476*, 2019.
- [26] Ian J Goodfellow, Mehdi Mirza, Da Xiao, Aaron Courville, and Yoshua Bengio. An empirical investigation of catastrophic forgetting in gradient-based neural networks. *arXiv preprint arXiv:1312.6211*, 2013.
- [27] Tyler L Hayes, Nathan D Cahill, and Christopher Kanan. Memory efficient experience replay for streaming learning. In *2019 International Conference on Robotics and Automation (ICRA)*, pages 9769–9776. IEEE, 2019.

- [28] Tyler L Hayes and Christopher Kanan. Lifelong machine learning with deep streaming linear discriminant analysis. *arXiv preprint arXiv:1909.01520*, 2019.
- [29] Alexander Hinneburg, Charu C. Aggarwal, and Daniel A. Keim. What is the nearest neighbor in high dimensional spaces? In *Proceedings of the 26th International Conference on Very Large Data Bases, VLDB '00*, pages 506–515, San Francisco, CA, USA, 2000. Morgan Kaufmann Publishers Inc.
- [30] Devon Hjelm, Alex Fedorov, Samuel Lavoie-Marchildon, Karan Grewal, Phil Bachman, Adam Trischler, and Yoshua Bengio. Learning deep representations by mutual information estimation and maximization. In *ICLR 2019*. ICLR, April 2019.
- [31] Yen-Chang Hsu, Yen-Cheng Liu, Anita Ramasamy, and Zsolt Kira. Re-evaluating continual learning scenarios: A categorization and case for strong baselines. In *NeurIPS Continual learning Workshop*, 2018.
- [32] Gabriel Huang, Hugo Larochelle, and Simon Lacoste-Julien. Centroid networks for few-shot clustering and unsupervised few-shot classification. *arXiv preprint arXiv:1902.08605*, 2019.
- [33] X. Ji, J. Henriques, and A. Vedaldi. Invariant information clustering for unsupervised image classification and segmentation. In *Proceedings of the International Conference on Computer Vision (ICCV)*, 2019.
- [34] Zhuxi Jiang, Yin Zheng, Huachun Tan, Bangsheng Tang, and Hanning Zhou. Variational deep embedding: An unsupervised and generative approach to clustering. In *Proceedings of the 26th International Joint Conference on Artificial Intelligence, IJCAI'17*, page 1965–1972. AAAI Press, 2017.
- [35] Zhuxi Jiang, Yin Zheng, Huachun Tan, Bangsheng Tang, and Hanning Zhou. Variational deep embedding: An unsupervised and generative approach to clustering. In *Proceedings of the 26th International Joint Conference on Artificial Intelligence, IJCAI'17*, pages 1965–1972. AAAI Press, 2017.
- [36] Ronald Kemker and Christopher Kanan. Fearnnet: Brain-inspired model for incremental learning. *International Conference on Learning Representations (ICLR)*, 2018.
- [37] Ronald Kemker, Marc McClure, Angelina Abitino, Tyler Hayes, and Christopher Kanan. Measuring catastrophic forgetting in neural networks. *AAAI Conference on Artificial Intelligence*, 2018.
- [38] Diederik P Kingma and Jimmy Ba. Adam: A method for stochastic optimization. *arXiv preprint arXiv:1412.6980*, 2014.
- [39] Diederik P. Kingma, Danilo J. Rezende, Shakir Mohamed, and Max Welling. Semi-supervised learning with deep generative models. In *Proceedings of the 27th International Conference on Neural Information Processing Systems - Volume 2, NIPS'14*, pages 3581–3589, Cambridge, MA, USA, 2014. MIT Press.
- [40] Diederik P Kingma and Max Welling. Auto-encoding variational bayes. *arXiv preprint arXiv:1312.6114*, 2013.
- [41] James Kirkpatrick, Razvan Pascanu, Neil Rabinowitz, Joel Veness, Guillaume Desjardins, Andrei A Rusu, Kieran Milan, John Quan, Tiago Ramalho, Agnieszka Grabska-Barwinska, et al. Overcoming catastrophic forgetting in neural networks. *Proceedings of the national academy of sciences*, 2017.
- [42] Adam Kosiorek, Hyunjik Kim, Yee Whye Teh, and Ingmar Posner. Sequential attend, infer, repeat: Generative modelling of moving objects. In S. Bengio, H. Wallach, H. Larochelle, K. Grauman, N. Cesa-Bianchi, and R. Garnett, editors, *Advances in Neural Information Processing Systems 31*, pages 8606–8616. Curran Associates, Inc., 2018.
- [43] Adam Kosiorek, Sara Sabour, Yee Whye Teh, and Geoffrey E Hinton. Stacked capsule autoencoders. In *Advances in Neural Information Processing Systems*, pages 15486–15496, 2019.

- [44] Dharshan Kumaran, Demis Hassabis, and James L McClelland. What learning systems do intelligent agents need? complementary learning systems theory updated. *Trends in cognitive sciences*, 20(7):512–534, 2016.
- [45] Chia-Wen Kuo, Chih-Yao Ma, Jia-Bin Huang, and Zsolt Kira. Manifold graph with learned prototypes for semi-supervised image classification. *arXiv preprint arXiv:1906.05202*, 2019.
- [46] Y. Lecun, L. Bottou, Y. Bengio, and P. Haffner. Gradient-based learning applied to document recognition. *Proceedings of the IEEE*, 86(11):2278–2324, Nov 1998.
- [47] Dong-Hyun Lee. Pseudo-label : The simple and efficient semi-supervised learning method for deep neural networks. *ICML 2013 Workshop : Challenges in Representation Learning (WREPL)*, 07 2013.
- [48] Kibok Lee, Kimin Lee, Jinwoo Shin, and Honglak Lee. Overcoming catastrophic forgetting with unlabeled data in the wild. In *Proceedings of the IEEE International Conference on Computer Vision*, pages 312–321, 2019.
- [49] Soochan Lee, Junsoo Ha, Dongsu Zhang, and Gunhee Kim. A neural dirichlet process mixture model for task-free continual learning. *arXiv preprint arXiv:2001.00689*, 2020.
- [50] Yanchao Li, Yongli Wang, Qi Liu, Cheng Bi, Xiaohui Jiang, and Shurong Sun. Incremental semi-supervised learning on streaming data. *Pattern Recognition*, 88, 11 2018.
- [51] Zhizhong Li and Derek Hoiem. Learning without forgetting. *IEEE transactions on pattern analysis and machine intelligence*, 40(12):2935–2947, 2017.
- [52] Xialei Liu, Chenshen Wu, Mikel Menta, Luis Herranz, Bogdan Raducanu, Andrew D Bagdanov, Shangling Jui, and Joost van de Weijer. Generative feature replay for class-incremental learning. *arXiv preprint arXiv:2004.09199*, 2020.
- [53] Vincenzo Lomonaco and Davide Maltoni. Core50: a new dataset and benchmark for continuous object recognition. *arXiv preprint arXiv:1705.03550*, 2017.
- [54] H. R. Loo and M. N. Marsono. Online data stream classification with incremental semi-supervised learning. In *Proceedings of the Second ACM IKDD Conference on Data Sciences, CoDS '15*, page 132–133, New York, NY, USA, 2015. Association for Computing Machinery.
- [55] David Lopez-Paz and Marc’Aurelio Ranzato. Gradient episodic memory for continual learning. In *Proceedings of the 31st International Conference on Neural Information Processing Systems, NIPS’17*, pages 6470–6479, USA, 2017. Curran Associates Inc.
- [56] Davide Maltoni and Vincenzo Lomonaco. Continuous learning in single-incremental-task scenarios. *Neural Networks*, 116:56–73, 2019.
- [57] Takeru Miyato, Shin-ichi Maeda, Shin Ishii, and Masanori Koyama. Virtual adversarial training: a regularization method for supervised and semi-supervised learning. *IEEE transactions on pattern analysis and machine intelligence*, 2018.
- [58] Yuval Netzer, Tao Wang, Adam Coates, Alessandro Bissacco, Bo Wu, and Andrew Y. Ng. Reading digits in natural images with unsupervised feature learning. In *NIPS Workshop on Deep Learning and Unsupervised Feature Learning 2011*, 2011.
- [59] Avital Oliver, Augustus Odena, Colin A Raffel, Ekin Dogus Cubuk, and Ian Goodfellow. Realistic evaluation of deep semi-supervised learning algorithms. In *Advances in Neural Information Processing Systems*, pages 3235–3246, 2018.
- [60] Aaron van den Oord, Yazhe Li, and Oriol Vinyals. Representation learning with contrastive predictive coding. *arXiv preprint arXiv:1807.03748*, 2018.
- [61] S.J. Pan and Q. Yang. A Survey on Transfer Learning. *IEEE Transactions on Knowledge and Data Engineering*, 22(10):1345–1359, 2010.

- [62] German I. Parisi, Ronald Kemker, Jose L. Part, Christopher Kanan, and Stefan Wermter. Continual lifelong learning with neural networks: A review. *Neural Networks*, 113:54 – 71, 2019.
- [63] German I Parisi, Jun Tani, Cornelius Weber, and Stefan Wermter. Lifelong learning of spatiotemporal representations with dual-memory recurrent self-organization. *Frontiers in neurorobotics*, 12:78, 2018.
- [64] Cengiz Pehlevan, Alexander Genkin, and Dmitri B Chklovskii. A clustering neural network model of insect olfaction. In *2017 51st Asilomar Conference on Signals, Systems, and Computers*, pages 593–600. IEEE, 2017.
- [65] Dushyant Rao, Francesco Visin, Andrei Rusu, Razvan Pascanu, Yee Whye Teh, and Raia Hadsell. Continual unsupervised representation learning. In *Advances in Neural Information Processing Systems 32*, pages 7645–7655. Curran Associates, Inc., 2019.
- [66] Antti Rasmus, Mathias Berglund, Mikko Honkala, Harri Valpola, and Tapani Raiko. Semi-supervised learning with ladder networks. In C. Cortes, N. D. Lawrence, D. D. Lee, M. Sugiyama, and R. Garnett, editors, *Advances in Neural Information Processing Systems 28*, pages 3546–3554. Curran Associates, Inc., 2015.
- [67] Sylvestre-Alvise Rebuffi, Alexander Kolesnikov, Georg Sperl, and Christoph H. Lampert. icarl: Incremental classifier and representation learning. In *2017 IEEE Conference on Computer Vision and Pattern Recognition, CVPR’17*, pages 5533–5542, 2017.
- [68] Mengye Ren, Eleni Triantafillou, Sachin Ravi, Jake Snell, Kevin Swersky, Joshua B. Tenenbaum, Hugo Larochelle, and Richard S. Zemel. Meta-learning for semi-supervised few-shot classification. In *Proceedings of 6th International Conference on Learning Representations ICLR*, 2018.
- [69] Sebastian Ruder. An overview of multi-task learning in deep neural networks. *arXiv preprint arXiv:1706.05098*, 2017.
- [70] Andrei A Rusu, Neil C Rabinowitz, Guillaume Desjardins, Hubert Soyer, James Kirkpatrick, Koray Kavukcuoglu, Razvan Pascanu, and Raia Hadsell. Progressive neural networks. *arXiv preprint arXiv:1606.04671*, 2016.
- [71] Hanul Shin, Jung Kwon Lee, Jaehong Kim, and Jiwon Kim. Continual learning with deep generative replay. In I. Guyon, U. V. Luxburg, S. Bengio, H. Wallach, R. Fergus, S. Vishwanathan, and R. Garnett, editors, *Advances in Neural Information Processing Systems 30*, pages 2990–2999. Curran Associates, Inc., 2017.
- [72] Jake Snell, Kevin Swersky, and Richard Zemel. Prototypical networks for few-shot learning. In *Advances in neural information processing systems*, pages 4077–4087, 2017.
- [73] Kihyuk Sohn, David Berthelot, Chun-Liang Li, Zizhao Zhang, Nicholas Carlini, Ekin D Cubuk, Alex Kurakin, Han Zhang, and Colin Raffel. Fixmatch: Simplifying semi-supervised learning with consistency and confidence. *arXiv preprint arXiv:2001.07685*, 2020.
- [74] Jost Tobias Springenberg. Unsupervised and semi-supervised learning with categorical generative adversarial networks. *arXiv preprint arXiv:1511.06390*, 2015.
- [75] Antti Tarvainen and Harri Valpola. Mean teachers are better role models: Weight-averaged consistency targets improve semi-supervised deep learning results. In I. Guyon, U. V. Luxburg, S. Bengio, H. Wallach, R. Fergus, S. Vishwanathan, and R. Garnett, editors, *Advances in Neural Information Processing Systems 30*, pages 1195–1204. Curran Associates, Inc., 2017.
- [76] Michael Tschanen, Olivier Bachem, and Mario Lucic. Recent advances in autoencoder-based representation learning. *arXiv preprint arXiv:1812.05069*, 2018.
- [77] Gido M van de Ven and Andreas S Tolias. Three scenarios for continual learning. *arXiv preprint arXiv:1904.07734*, 2019.

- [78] Rajasekar Venkatesan and Meng Joo Er. A novel progressive learning technique for multi-class classification. *Neurocomput.*, 207(C):310–321, September 2016.
- [79] Junyuan Xie, Ross Girshick, and Ali Farhadi. Unsupervised deep embedding for clustering analysis. In Maria Florina Balcan and Kilian Q. Weinberger, editors, *Proceedings of The 33rd International Conference on Machine Learning*, volume 48 of *Proceedings of Machine Learning Research*, pages 478–487, New York, New York, USA, 20–22 Jun 2016. PMLR.
- [80] Jianwei Yang, Devi Parikh, and Dhruv Batra. Joint unsupervised learning of deep representations and image clusters. In *Proceedings of the IEEE Conference on Computer Vision and Pattern Recognition*, pages 5147–5156, 2016.
- [81] Suet-Peng Yong, Jeremiah D. Deng, and Martin K. Purvis. Novelty detection in wildlife scenes through semantic context modelling. *Pattern Recogn.*, 45(9):3439–3450, September 2012.
- [82] Jaehong Yoon, Eunho Yang, Jeongtae Lee, and Sung Ju Hwang. Lifelong learning with dynamically expandable networks. In *International Conference on Learning Representations*, 2018.
- [83] Jason Yosinski, Jeff Clune, Yoshua Bengio, and Hod Lipson. How transferable are features in deep neural networks? In Z. Ghahramani, M. Welling, C. Cortes, N. D. Lawrence, and K. Q. Weinberger, editors, *Advances in Neural Information Processing Systems 27*, pages 3320–3328. Curran Associates, Inc., 2014.
- [84] Friedemann Zenke, Ben Poole, and Surya Ganguli. Continual learning through synaptic intelligence. In *International Conference on Machine Learning*, 2017.
- [85] Chen Zeno, Itay Golan, Elad Hoffer, and Daniel Soudry. Task agnostic continual learning using online variational bayes. *arXiv preprint arXiv:1803.10123*, 2018.
- [86] Guanyu Zhou, Kihyuk Sohn, and Honglak Lee. Online incremental feature learning with denoising autoencoders. In Neil D. Lawrence and Mark Girolami, editors, *Proceedings of the Fifteenth International Conference on Artificial Intelligence and Statistics*, volume 22 of *Proceedings of Machine Learning Research*, pages 1453–1461, La Palma, Canary Islands, 21–23 Apr 2012. PMLR.

## SUPPLEMENTARY MATERIAL

### A STAM Notation and Hyperparameters

All STAM notation and parameters are listed in Tables 1-4.

**Table 1:** STAM Notation

Symbol	Description
$\mathbf{x}$	input vector.
$n$	dimensionality of input data
$M_l$	number of patches at layer $l$ (index: $m = 1 \dots M_l$ )
$\mathbf{x}_{l,m}$	$m$ 'th input patch at layer $l$
$C_l$	set of centroids at layer $l$
$\mathbf{c}_{l,j}$	centroid $j$ at layer $l$
$d(\mathbf{x}, c)$	distance between an input vector $\mathbf{x}$ and a centroid $c$
$\hat{c}(\mathbf{x})$	index of nearest centroid for input $x$
$\tilde{d}_l$	novelty detection distance threshold at layer $l$
$U(t)$	the set of classes seen in the unlabeled data stream up to time $t$
$L(t)$	the set of classes seen in the labeled data up to time $t$
$k$	index for representing a class
$g_{l,j}(k)$	association between centroid $j$ at layer $l$ and class $k$ .
$D_l$	average distance between a patch and its nearest neighbor centroid at layer $l$ .
$v_{l,m}(k)$	vote of patch $m$ at layer $l$ for class $k$
$v_l(k)$	vote of layer $l$ for class $k$
$k(\mathbf{x})$	true class label of input $x$
$\hat{k}(\mathbf{x})$	inferred class label of input $x$
$\Phi(\mathbf{x})$	embedding vector of input $x$

**Table 2:** STAM Hyperparameters

Symbol	Default	Description
$\Lambda$	3	number of layers (index: $l = 1 \dots \Lambda$ )
$\alpha$	0.1	centroid learning rate
$\beta$	0.95	percentile for novelty detection distance threshold
$\gamma$	0.15	used in definition of class informative centroids
$\Delta$	see below	STM capacity
$\theta$	30	number of updates for memory consolidation
$\rho_l$	see below	patch dimension

**Table 3:** MNIST/EMNIST Architecture

Layer	$\rho_l$	$\Delta$ (incremental)	$\Delta$ (uniform)
1	8	400	2000
2	13	400	2000
3	20	400	2000

**Table 4:** SVHN Architecture

Layer	$\rho_l$	$\Delta$ (incremental)	$\Delta$ (uniform)
1	10	2000	10000
2	14	2000	10000
3	18	2000	10000

### B Baseline models

The first baseline is a convolutional autoencoder (CAE) architecture trained to optimize Euclidean reconstruction error – see Table SM-5. It is trained using Adam optimization [38] with a learning rate of  $10^{-4}$  and no decay. The encoder consists of three convolution layers with ReLU activations,

embedding inputs into a 64-dimension latent space. The decoder consists of three transposed convolution layers with ReLU activations. The final layer uses linear activations. The representations at the 64-dimension latent space are used to perform the clustering and classification tasks. The details of the CAE architecture are given in Table 5. FC denotes fully connected layers, and Conv\_Trans denotes transposed convolution layers.

The second baseline is a self-supervised method which learns the auxiliary task of predicting image rotations [23]. We chose this approach because it has a stable loss function and it does not require data replay. The training data is augmented so that each training image is rotated by 0, 90, 180 and 270 degrees. The network is trained by minimizing the cross-entropy loss on a four-way classification task of predicting the rotation of the training images. The model uses a *network-in-network* architecture with five *conv-blocks*, where each conv-block consists of three convolutional layers. We train the network with SGD with a batch size of four (the four rotations of a single training image in the original data set) and with one epoch, again to only process each unlabeled example once. The momentum is set to 0.9 and the learning rate to 0.1. In order to perform clustering and classification we generate a feature map from the outputs of the network’s second conv-block, which produces the best features for downstream tasks according to [23].

The third baseline is Principal Component Analysis (PCA). This dimensionality reduction method serves as a simple baseline that is not based on deep learning. In all three tasks, we utilize PCA to project the data onto an  $m$ -dimensional orthogonal subspace. We perform the classification tasks by using the embedding of each image as input to a K-Nearest Neighbors classifier. We perform the clustering task by using the embedding as input to K-Means. The dimension  $m$  is set to the minimum between the smallest dimension of the data matrix and the number of dimensions that explain 90% of the variance. These values are 300, 150, 50 for MNIST, EMNIST, and SVHN, respectively. The number of components for MNIST is 20, 40, 60, 80, and 100 in phases 1, 2, 3, 4, and 5, respectively. Similarly for EMNIST, the value is increasing by twenty in every phase until phase 8, where it exceeds the value that represents 90% of the variance (150).

**Table 5:** CAE Architecture

Encoder					
Layer Type	# Filters	Kernel Size	Stride	# Units	Activation Unit
Conv	128	3	1	-	ReLU
Conv	64	3	2	-	ReLU
Conv	32	3	2	-	ReLU
FC	-	-	-	1568	ReLU
FC	-	-	-	64	Sigmoid
Decoder					
Layer Type	# Filters	Kernel Size	Stride	# Units	Activation Unit
FC	-	-	-	1568	ReLU
Conv_Trans	128	3	1	-	ReLU
Conv_Trans	64	3	2	-	ReLU
Conv_Trans	32	3	2	-	ReLU
Conv_Trans	1	1	1	-	Linear

### C A closer look at STAM in Incremental UPL

We refer the reader to Figure 6. As we introduce new classes to the incremental UPL stream, the architecture recognizes previously learned classes without any major degradation in classification accuracy (left column). The average accuracy per phase is decreasing, which is due to the increasingly difficult expanding classification task. For EMNIST, we only show the average accuracy because there are 47 total classes. In all datasets, we observe that layer-2 and layer-3 (corresponding to the largest two receptive fields) contain the highest fraction of CIN centroids (center column). The ability to recognize new classes is perhaps best visualized in the LTM centroid count (right column). During each phase the LTM count stabilizes until a sharp spike occurs at the start of the next phase when new classes are introduced. This reinforces the claim that the LTM pool of centroids (i) is stable when there are no new classes, and (ii) is able to recognize new classes via novelty detection when they appear. In the EMNIST experiment, as the number of classes increases towards 47, we gradually



see fewer “spikes” in the LTM centroids for the lower receptive fields, which is expected given the repetition of patterns at that small patch size. However, the highly CIN layers 2 and 3 continue to recognize new classes and create centroids, even when the last few classes are introduced.

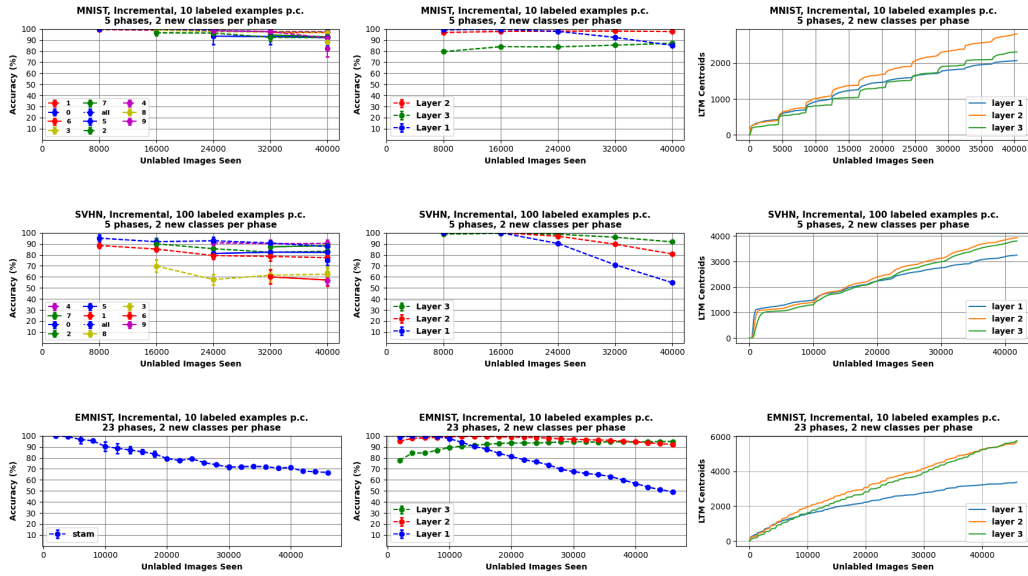


**Figure 6:** STAM Incremental UPL evaluation for MNIST (row-1), SVHN (row-2), and EMNIST (row-3). Per-class and average classification accuracy (left); number of LTM centroids over time (center); fraction of CIN centroids over time (right). The task is expanding classification, i.e., recognize all classes seen so far.

## D Effect of unlabeled and labeled data on STAM

We next examine the effects of unlabeled and labeled data on the STAM architecture (Figure 7). As we vary the length of the unlabeled data stream (left), we see that STAMs can actually perform well even with much less unlabeled data. This suggests that the STAM architecture may be applicable even where the datastream is much shorter than in the experiments of this paper. A longer stream would be needed however if there are many classes and some of them are infrequent. The accuracy “saturation” observed by increasing the unlabeled data from 20000 to 60000 can be explained based on the memory mechanism, which does not update centroids after they move to LTM. As showed in the ablation studies, this is necessary to avoid forgetting classes that no longer appear in the stream. The effect of varying the number of labeled examples per class (right) is much more pronounced. We see that the STAM architecture can perform well above chance even in the extreme case of only a single (or small handful of) labeled examples per class.

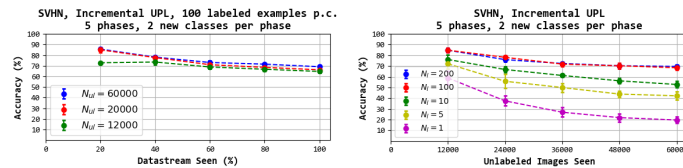


**Figure 7:** The effect of varying the amount of unlabeled data in the entire stream (left) and labeled data per class (right).

## E STAM Hyperparameter Sweeps

We examine the effects of STAM hyperparameters in Figure 8. (a) As we decrease the rate of  $\alpha$ , we see a degradation in performance. This is likely due to the static nature of the LTM centroids

- with low  $\alpha$  values, the LTM centroids will primarily represent the patch they were initialized as. (b) As we vary the rates of  $\gamma$ , there is little difference in our final classification rates. This suggests that the maximum  $g_{i,j}(k)$  values are quite high, which may not be the case in other datasets besides SVHN. (c) We observe that STAM is robust to changes in  $\Theta$ . (d,e) The STM size  $\Delta$  has a major effect on the number of learned LTM centroids and on classification accuracy. (e) The accuracy in phase-5 for different numbers of layer-3 LTM centroids (and corresponding  $\Delta$  values). The accuracy shows diminishing returns after we have about 1000 LTM centroids at layer-3. (g,h) As  $\beta$  increases the number of LTM centroids increases (due to a lower rate of novelty detection); if  $\beta \geq 0.9$  the classification accuracy is about the same.

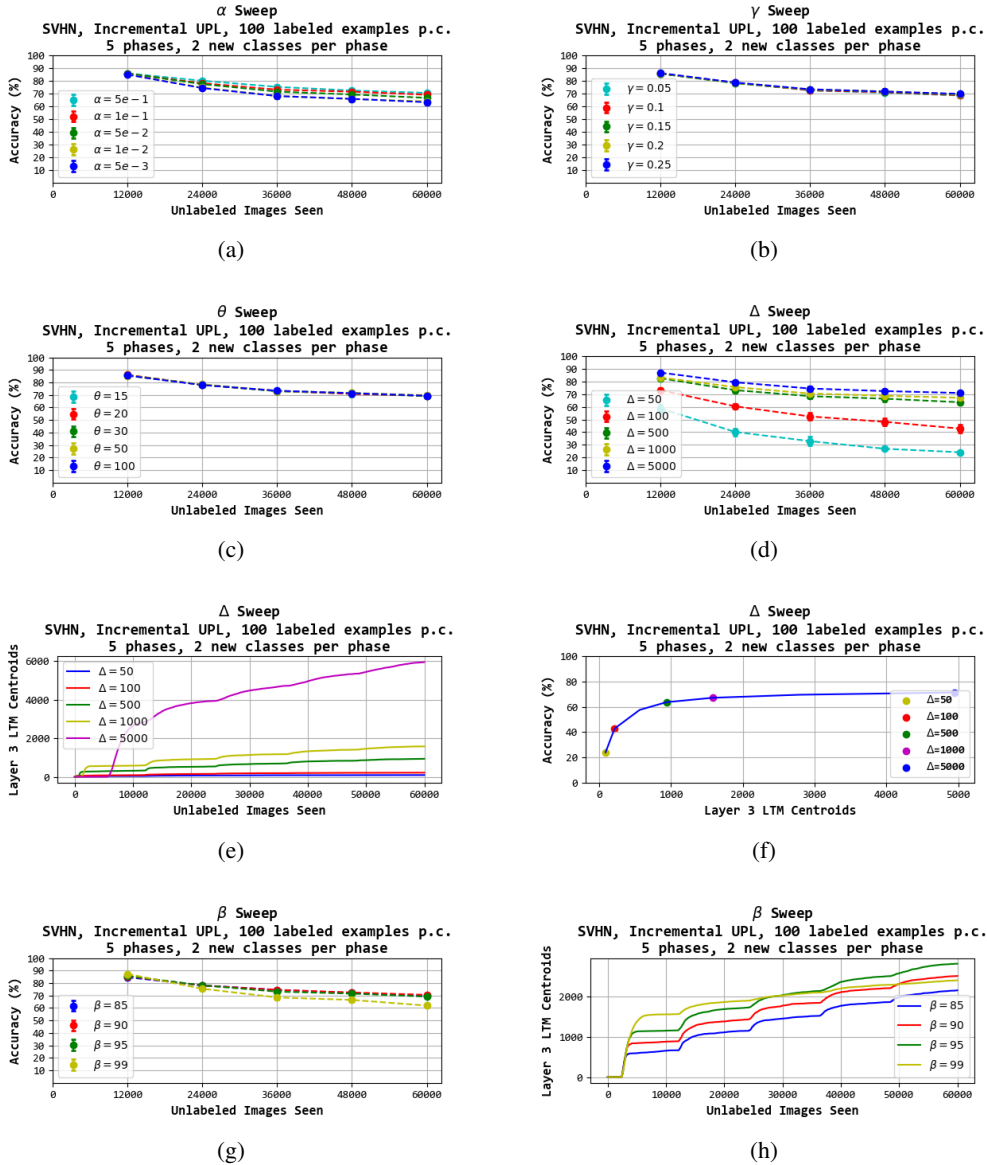
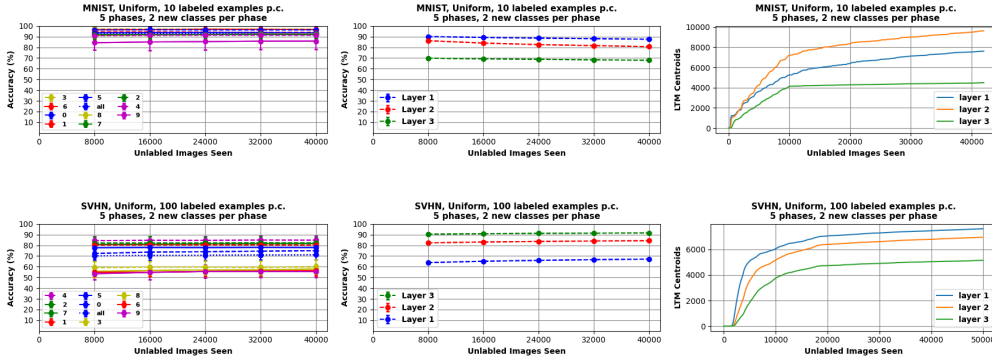


Figure 8: Hyperparameter sweeps for  $\alpha$ ,  $\gamma$ ,  $\theta$ ,  $\beta$ , and  $\Delta$ .

## F Uniform UPL

In order to examine if the STAM architecture can learn all classes simultaneously, but without knowing how many classes exist, we also evaluate the STAM architecture in a uniform UPL scenario

(Figure 9). Note that LTM centroids converge to a constant value, at least at the top layer, Each class is recognized at a different level of accuracy, depending on the similarity between that class and others.



**Figure 9:** Uniform UPL evaluation for MNIST (row-1) and SVHN (row-2). Per-class/average classification accuracy is given at the left; the number of LTM centroids over time is given at the center; the fraction of CIN centroids over time is given at the right.

## G Image preprocessing

Given that each STAM operates on individual image patches, we perform *patch normalization* rather than image normalization. We chose a normalization operation that helps to identify similar patterns despite variations in the brightness and contrast: every patch is transformed to zero-mean, unit variance before clustering. At least for the datasets we consider in this paper, grayscale images result in higher classification accuracy than color.

We have also experimented with ZCA whitening and Sobel filtering. ZCA whitening did not work well because it requires estimating a transformation from an entire image dataset (and so it is not compatible with the online nature of the UPL problem). Sobel filtering did not work well because STAM clustering works better with filled shapes rather than the fine edges produced by Sobel filters.

## H Memory footprint analysis

The memory requirement of the STAM model can be calculated as:

$$M = \sum_{l=1}^{\Lambda} \rho_l^2 \cdot (|C_l| + \Delta) \quad (8)$$

For the 3-layer SVHN architecture with  $|C_l| \approx 3000$  LTM centroids in every layer and  $\Delta = 2000$ , the memory footprint is 5,064,000 pixels, equivalent to roughly 5000 grayscale SVHN digits. This memory requirement can be significantly reduced however. Figure 8(f) shows that the accuracy remains almost the same when  $\Delta = 500$  and  $|C_l| \approx 1000$ . With these values the memory footprint reduces to about 950,000 pixels, equivalent to roughly 930 grayscale SVHN digits.

By comparison, the CAE architecture has 4,683,425 trainable parameters, which should be stored at floating-point precision. With four bytes per weight, then STAM model would require  $\frac{950000}{4683425 \times 4} \approx 5\%$  of the CAE’s memory footprint. Similarly, the RotNet architecture has 1,401,540 trainable parameters, which would also be stored at floating-point precision. Again, with four bytes per weight, the STAM model would require  $\frac{950000}{1401540 \times 4} \approx 17\%$  of RotNet’s memory footprint. Future work can decrease the STAM memory requirement further by merging similar LTM centroids.